Received: June 11, 2022. Revised: July 25, 2022.

INASS

International Journal of
Intelligent Engineering & Systems

http://www.inass.org/

Brain Tumor Detection by Modified Particle Swarm Optimization Algorithm and Multi-Support Vector Machine Classifier

Preethi Srinivasalu[1*] **Aishwarya Palaniappan[1]**

[1]*Atria Institute of Technology, Bengaluru, Karnataka 560024, India*
* Corresponding author's Email: preethi.srinivas2002@gmail.com

Abstract: In recent times, brain tumor detection become an important task in medical image processing applications. The early detection of brain tumor improves the treatment process and increases the survival rate of the patients. However, the manual segmentation and classification of brain tumor is a complex and time consuming process. Therefore, a new automatic brain tumor detection model is implemented in this manuscript for effective brain tumor detection. After collecting the scans from the cloud, the normalization and adaptive histogram equalization techniques are used to enhance the acquired brain scan quality. Further, the tumor regions are segmented by integrating the Adaptive Kernel Fuzzy C Means (AKFCM) clustering algorithm with the Otsu thresholding technique. Next, the deep and textual feature values are extracted from the segmented regions using the Gray Level Co-occurrence Matrix (GLCM), Local Ternary Pattern (LTP), and LeNet-5. The dimension of the extracted feature vectors is optimized by using the Modified Particle Swarm Optimization (MPSO) algorithm, which are given as the input to the Multi-Support Vector Machine (MSVM) for tumor classification. The experimental outcomes confirmed that the MPSO-MSVM model obtained high accuracy of 98.89%, which is superior related to the existing machine learning techniques.

Keywords: Brain tumor detection, Local ternary pattern, Magnetic resonance imaging, Multi-support vector machine, Particle swarm optimization.

1. Introduction

In recent decades, the timely diagnosis of the brain tumor is essential in terms of treatment planning and patient health [1, 2]. In addition, the valuation of Magnetic resonance imaging (MRI) is usually a complex and time-consuming mechanism for radiologists that pro-longs the treatment planning procedure and endangers the patient health [3-5]. Recently, computer aided automatic diagnostic methods have become popular in brain tumor detection [6]. The machine learning techniques are started to implement quite a lot in the medical image processing applications for classifying the brain tumor types [7, 8]. The robust machine learning techniques improve the diagnosis accuracy, which helps the clinicians/physicians to make final decisions [9, 10]. Brain tumor detection is still a challenging task, because the MRI scans are formed with the interactions of illumination changes [11], lighting variations [12], and background interferences [13]. The human ability to recognize the tumor regions in the MRI brain images is naturally significant, but it may not be precise all the time [14-15]. In this manuscript, an efficient machine learning based model is proposed for precise brain tumor detection. The major contributions of this manuscript are listed as follows:

- After the acquisition of images from T1-weighted contrast enhanced (CE) MRI dataset (standard cloud dataset), normalization and adaptive histogram equalization techniques are used for quality improvement. Further, tumor segmentation is accomplished by integrating both AKFCM and Otsu thresholding technique.
- Feature extraction is performed using GLCM, LTP, and LeNet-5 models that extract both texture and deep feature vectors. The combination of lower and higher-level feature vectors reduces the semantic space that helps in better classification.

- The developed MPSO algorithm for feature optimization decreases the system complexity and running time of the classifier. In the MPSO algorithm, linear decreasing inertia weight is used that improve the fine-tuning characteristics of the conventional PSO algorithm.
- The selected feature vectors are given as the input to the MSVM for classifying the tumor types. The MPSO-MSVM model's efficacy is investigated in light of the matthews correlation coefficient (MCC), specificity, sensitivity, f-score, and accuracy.

This manuscript is organized as follows: some manuscripts related to brain tumor detection are reviewed in section 2. Theoretical description and experimental evaluation of the MPSO-MSVM model are represented in sections 3 and 4. The conclusion of this manuscript is given in section 5.

2. Related works

Swati [16] presented a novel model based on transfer-learning and fine-tuning for MRI brain tumor detection. In this work, the pre-trained convolutional neural network (CNN) models such as adopted transfer-learning and visual geometry group (VGG) 19 were applied for extracting the feature values from the MRI brain scans. Additionally, a block wise fine-tuning was applied to obtain better classification results, where the block wise fine-tuning technique goes deep down into the CNN blocks for monitoring the performance improvement. The effectiveness of the presented model was investigated on the T1-CE MRI image dataset in terms of accuracy, f-score, specificity, and sensitivity. The experimental outcomes showed that the presented model not only outperformed the conventional machine learning techniques and standard CNN models on the T1-CE MRI image dataset. Díaz-Pernas [17] introduced a novel automated model based on deep CNN with multi-scale method for brain tumor detection and classification. Further, Sultan [18] implemented a deep learning model based on CNN for classifying different brain tumor types. In the resulting section, the CNN model achieved an efficient performance with better overall accuracy. The experimental outcome indicates the ability of the presented model for brain tumor multi-classification purposes. However, the computational time of the CNN model was high, if it has more layers.

Hashemzehi [19] integrated CNN and neural autoregressive distribution estimation (NADE) for automated brain tumor detection. The presented model superiorly extracts beneficial feature vectors, eliminates undesired feature vectors and smooths the boundary of the brain tumors for better image classification. The CNN model needs an enormous amount of data to perform better than the machine learning techniques which was a major concern in this literature. Kaplan [20] implemented two modified local binary patterns (LBP) descriptors like αLBP and nLBP for detecting the brain tumor types: pituitary, meningioma and glioma. The extracted feature vectors were fed to the classifiers such as random forest, K-nearest neighbor (KNN), linear discriminant analysis, and artificial neural networks for classification. The combination: of modified LBP feature descriptors with KNN obtained better classification accuracy related to other classifiers. However, the KNN needs prior knowledge about the problem domain which was a time consuming task. Ismael [21] presented a novel model to classify brain tumor types using residual networks. The developed model's effectiveness was evaluated on a benchmark dataset: T1-CE MRI in terms of f-score, precision, accuracy and recall. The increase in the network depth leads to the problems like vanishing gradients.

Rammurthy and Mahesh, [22] used rough set theory and cellular automata technique for segmenting the tumor regions from the acquired images. In addition, the local optimal oriented pattern, tumor size, mean, kurtosis, and variance were applied for extracting the features from the segmented regions. Next, the deep CNN model with whale harris hawks optimization (WHHO) algorithm was developed for brain tumor classification. Srikanth, and Suryanarayana, [23] implemented the VGG-16 model for multi-class classification of brain tumor MRI images. However, the deep CNN and VGG-16 models need expensive graphics processing units for data processing, which was computationally expensive.

Hapsari [24] implemented a new enCNN model based on VGG-16 for brain tumor classification. The enCNN model includes 7 convolutional layers, 4 max pooling and ReLU layers. Additionally, an optimizer was used for fine tuning the hyper-parameters in order to predict the class performance. As specified earlier, the CNN model was computationally costly. Alnaggar [25] has integrated chimp optimization algorithm (COA) and CNN model for effective brain tumor segmentation. As seen in the resulting section, the computational time was higher compared to the existing models. To highlight the aforementioned problems, a new model: MPSO-MSVM is introduced in this manuscript for effective brain tumor detection.

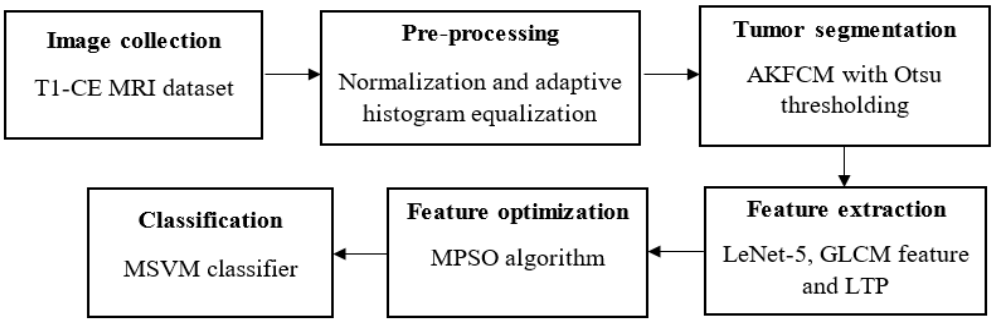

Figure 1. Flowchart of the MPSO-MSVM model

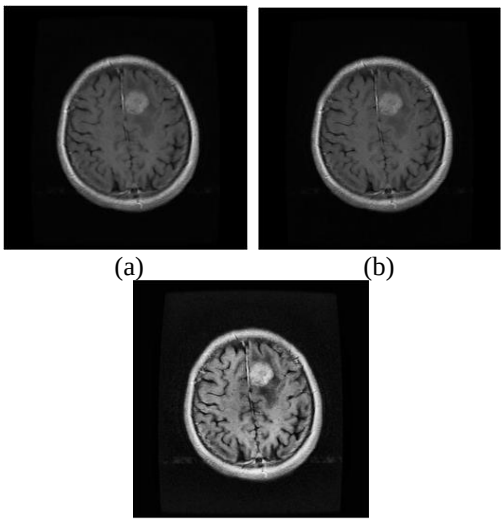

(a) (b)

(c)

Figure. 2 :(a) Original image, (b) normalized image and (c) enhanced image

3. Methodology

In the brain tumor detection, the proposed MPSO-MSVM model includes six phases: image collection: T1-CE MRI dataset, preprocessing: normalization and adaptive histogram equalization, tumor segmentation: AKFCM with Otsu thresholding, feature extraction: LeNet-5, GLCM feature, and LTP, feature optimization: MPSO, and tumor classification: MSVM. The flowchart of the MPSO-MSVM model is given in Fig. 1.

3.1 Image collection and pre-processing

In the starting phase of brain tumor detection, the brain images are acquired from the standard cloud dataset named T1-CE MRI. The T1-CE MRI dataset comprises 3064 brain scans, which are acquired from 233 subjects and it includes 3 types of brain tumors such as glioma (1426 slices), meningioma (708 slices), and pituitary tumor (930 slices) [26]. The sample image of T1-CE MRI dataset is graphically denoted in Fig. 2. After the collection of brain images, image normalization and adaptive histogram equalization techniques are employed to enhance the quality of the collected brain image. The adaptive histogram equalization technique adjusts the image contrast by utilizing its histogram value. This technique stretches the intensity range of the images or spreads the most frequent pixel intensity values for enhancing the contrast of the acquired brain scans. Additionally, the normalization alters the pixel value range for contrast stretching. The mathematical expression of the image normalization technique is determined in Eq. (1).

$$IN = (I - Min) \times \frac{newMax - newMin}{Max - Min} + newMin \quad (1)$$

Where, IN indicates normalized brain images, I states original brain images, $Min\ and\ Max$ states minimum and maximum pixel value. The normalized and enhanced images are graphically defined in Fig. 2.

3.2 Tumor segmentation

After pre-processing the brain scans, the AKFCM with Otsu thresholding technique is applied to segment the tumor regions. The selection of the clustering centroids is essential for an effective segmentation result. Several clustering algorithms are developed by setting the clustering centroids artificially based on prior knowledge. The clustering centroids should update iteratively to enhance the segmentation effect and further, updated the centroids until the best cluster segmentation result is obtained. The systematic process of the AKFCM clustering algorithm is given below [27],

Step 1: Set the convergence condition, initial clustering centroid, cluster number, and total number of the neighborhood pixel in the filtering window.

Step 2: Estimate the adaptive weighting means of the filtered image.

Step 3: Determine the best membership function.

Step 4: Reduce the objective function by utilizing the clustering centroids and the best membership function.

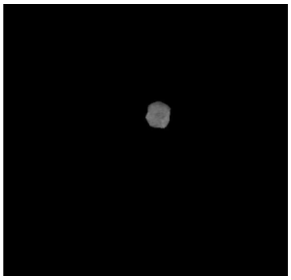

Figure. 3 Segmented image with tumor region

Step 5: Compute the absolute value.

Step 6: The clustering segmentation is finished based on the best membership degree rules. Next, the segmented images are given as the input to the Otsu thresholding for effective segmentation of the tumor regions.

The Otsu thresholding works based on discriminate analysis to determine the maximum separability of the tumor classes. Based on the image thresholding, the Otsu thresholding technique performs an automatic histogram shape. Firstly, the Otsu thresholding technique assumes the clustered images for tumor segmentation that comprises of the foreground region f_r and background region b_r. By utilizing the discrete probability density function, the Otsu thresholding constructs normalized histogram that is mathematically represented in Eq. (2).

$$p_r(r_q) = \frac{s_q}{s}, q = 0,1,2, \ldots\ldots, h-1 \quad (2)$$

Where, h states maximum intensity level of the clustered images, s denotes total number of pixels in the clustered images, s_q specifies the pixel value, which has an intensity level r_q.

The initial threshold value is the mid-point between the minimum and maximum intensity values of the clustered brain scans. If o is considered as an initial threshold value, then f_r indicates the pixel-sets with the levels $[0, 1, \ldots o-1]$ and b_r specifies the pixel-sets with the levels $[o, o+1, \ldots h-1]$. The Otsu thresholding technique selects the optimal threshold value o^* that increases the between-class variance σ^2, which is defined in Eqs. (3) and (4). The segmented image is graphically depicted in Fig. 3.

$$\sigma^2 = e_0, e_0 = \sum_{q=0}^{o-1} p_q(r_q) \quad (3)$$

Where,

$$\sigma^2(o^*) = \frac{arg}{0<o<h-1} max\sigma^2(o) \quad (4)$$

3.3 Feature extraction and optimization

After segmenting the tumor regions, the feature extraction is carried-out utilizing LTP, GLCM features (contrast, homogeneity, energy and correlation), and LeNet-5. The LTP is an extension of the local binary pattern, which is more robust to the noise. In the LTP descriptor, the LBP is extended to three valued codes to extract the textual feature values from the segmented regions. Further, the GLCM features: contrast, homogeneity, energy, and correlation are texture feature descriptors that are applied for estimating the second order properties of the brain images. The GLCM features provide information about the relative position of the neighborhood image pixels in the segmented tumor regions. Correspondingly, the LeNet-5 model comprises two sets of average pooling and convolutional layers followed by flattening convolutional layer and two fully connected layers for extracting the deep feature vectors. The parameter setting of the LeNet-5 model is listed as follows: minimum batch size is 4, validation frequency is 20, maximum epochs is 100, and the initial learning rate is 0.001. By using feature level fusion, the extracted feature vectors of LTP, GLCM features, and LeNet-5 are combined, which is 612 feature vectors.

The extracted feature vectors are optimized by using the MPSO algorithm that helps in improving the system complexity and computational time. The traditional PSO algorithm is inspired by the behaviors of bird flocking and fish schooling. Generally, the bird searches food by moving from one place to another place and by smelling it finds the food. While searching food, the bird is aware of its location, which helps in identifying and managing the food resources. The learning procedure is determined by estimating the crowd or swarm, which is technically called as particle. In the crowd, the PSO algorithm finds the partner position to search the space globally and then the velocity v_{id} and position x_{id} of the particles are updated by utilizing the Eqs. (5) and (6).

$$v_{id}(t+1) = w \times v_{id}(t) + c_1 \times r_1 \times [p_{id}(t) - x_{id}(t)] + c_2 \times r_2 \times [p_{gd}(t) - x_{id}(t)] \quad (5)$$

$$x_{id}(t+1) = x_{id}(t) + v_{id}(t+1) \quad (6)$$

Where, w indicates inertia weight, which balances the global and local search, c_1 and c_2 represents acceleration coefficients, and r_1 and r_2 denotes two random numbers, which are distributed in the range of 0 to 1. In addition, p_{id} and p_{gd} are represented as particles' current best position and global best position.

A new linear decreasing inertia weight $w(t)$ is used in the MPSO algorithm, which improves the fine-tuning characteristics of the traditional PSO algorithm. In the MPSO algorithm, the inertia weight $w(t)$ minimized from the initial value w_{max} to the final value w_{min}, when iteration increases. A new linear decreasing inertia weight $w(t)$ is expressed in Eq. (7).

$$w(t) = \frac{t_{max}-t}{t_{max}}(w_{max} - w_{min}) + w_{min} \quad (7)$$

The parameter setting of the MPSO algorithm is listed as follows: population size is equal to the total extracted feature vectors, maximum number of iteration t is 100, cognitive constant c_1 is 2 and social constant c_2 is 2. The optimized 300 feature vectors are fed to the MSVM for classifying the tumor types such as glioma, meningioma, and pituitary tumor.

3.4 Tumor classification

The optimized 300 feature vectors are given as the input to the MSVM classification technique for tumor classification. In medical image processing applications, the traditional SVM method is used only for binary class classification, so it is necessary in creating a multi-SVM classification technique for multi-class classification. In the multi-class classification problems, the commonly employed approaches are one against all, and one against one. The MSVM classification technique generates all possible two-class classifiers from the training sets of n^{th} classes, and it trains only two out of the n^{th} classes, which results in $n \times (n-1)/2$ classifiers. In the MSVM classification technique, the decision function is an active way for moderating the multi-class problems, which is constructed by assuming all the n^{th}classes. The M-SVM classification technique is an extension of SVM that is mathematically specified in the Eqs. (8), (9), and (10).

$$min\Phi(wn, \xi) = 1/2 \sum_{m=1}^{k}(wn_m) + p_c \sum_{i=1}^{l}\sum_{m \neq yi} \xi_i^m \quad (8)$$

Subjected to,

$$\left(wn_{yi} \times z_i\right) + b_{yi} \geq \left(wn_{yi} \times z_i\right) + b_m + 2 - \xi_i^m, \quad (9)$$

$$\xi_i^m \geq 0, i = 1,2,3 \ldots l, m, yi \in \{1,2,3 \ldots k\}, m \neq yi \quad (10)$$

Where, l indicates training data point, ξ_i^m denotes slack variables, wn represents weights that meet the requirements of a probability distribution, p_c denotes user positive constant, yi represents class of training data vectors z_i, and $k = 3$ states number of classes. At last, the decision function is stated in Eq. (11). In the MSVM classifier, the standardize is fixed as true, and the kernel function is linear.

$$f(z) = arg\,max[(wn_i \times z) + b_i], \quad i = 1,2,3,..k \quad (11)$$

4. Experimental results

In the brain tumor detection, the MPSO-MSVM model is simulated by using MATLAB 2020 software environment on a system configuration with windows 10 operating system, 16GB random access memory and Intel core i9 processor. In this scenario, the effectiveness of the MPSO-MSVM model is tested in light of MCC, specificity, sensitivity, f-score, and accuracy. The value range of MCC lies between +1 to -1, where a model with a score of -1 is a poor model and a model with a score of +1 is a perfect model for brain tumor detection. In addition, the specificity is called a true negative rate, which is the proportion of negative rates that are accurately classified by MPSO-MSVM model. Correspondingly, the sensitivity is also called recall or true positive rate, which is the proportion of positive rates that are precisely classified by the proposed model. The formula to calculate MCC, specificity, and sensitivity is defined in the Eqs. (12-14).

$$MCC = \frac{TP \times TN - FP \times FN}{\sqrt{(TP+FP)(TP+FN)(TN+FP)(TN+FN)}} \times 100 \quad (12)$$

$$Specificity = \frac{TN}{TN+FP} \times 100 \quad (13)$$

$$Sensitivity = \frac{TP}{TP+FN} \times 100 \quad (14)$$

The f-score is a harmonic mean of precision and sensitivity, where it reaches the best value at one and the worst value at zero. The classification accuracy is the proportion of correct predictions among the total number of cases, where the predictions include both negative and positive values. Hence, the mathematical formula of f-score and accuracy is denoted in the Eqs. (15-16).

$$F - score = \frac{2TP}{FP+2TP+FN} \times 100 \quad (15)$$

$$Accuracy = \frac{TP+TN}{TP+TN+FP+FN} \times 100 \quad (16)$$

Table 1. Experimental result of different classifiers without using feature optimization

Without feature optimization					
Classifiers	**Accuracy (%)**	**Sensitivity (%)**	**Specificity (%)**	**F-score (%)**	**MCC (%)**
KNN	83.33	83.87	82.24	79.28	81.2
DNN	60.67	63.81	61.62	63.53	60.97
Random forest	93.33	89.78	92.67	90.3	92.9
Decision tree	83.23	82.39	81.73	82.62	83.78
MSVM	96.57	95.92	97.21	95.37	94.48

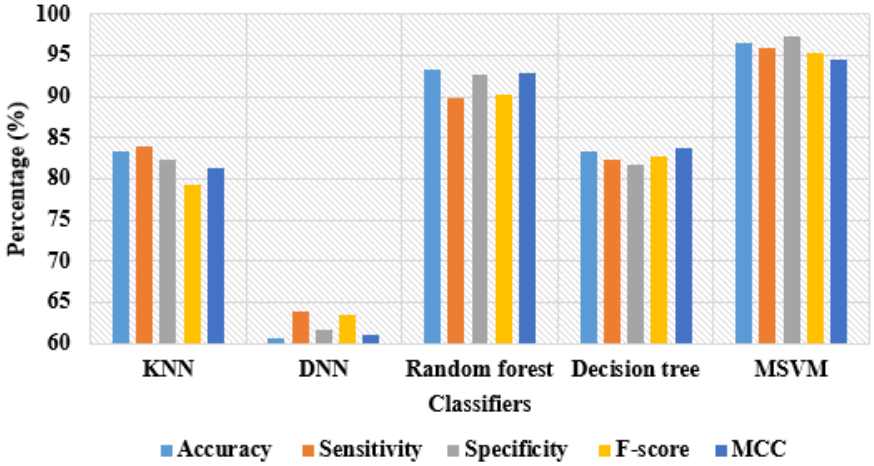

Figure. 3 The comparison result of different classifiers without using feature optimization

Table 2. Experimental result of different classifiers with MPSO algorithm

MPSO algorithm					
Classifiers	**Accuracy (%)**	**Sensitivity (%)**	**Specificity (%)**	**F-score (%)**	**MCC (%)**
KNN	93.33	89.78	92.67	90.30	89.53
DNN	66.61	65	63.57	63.33	66.36
Random forest	96.78	96.54	97.43	96.09	97.38
Decision tree	96.67	93.94	97.41	95.07	93.82
MSVM	98.89	98.65	97.54	98.32	97.02

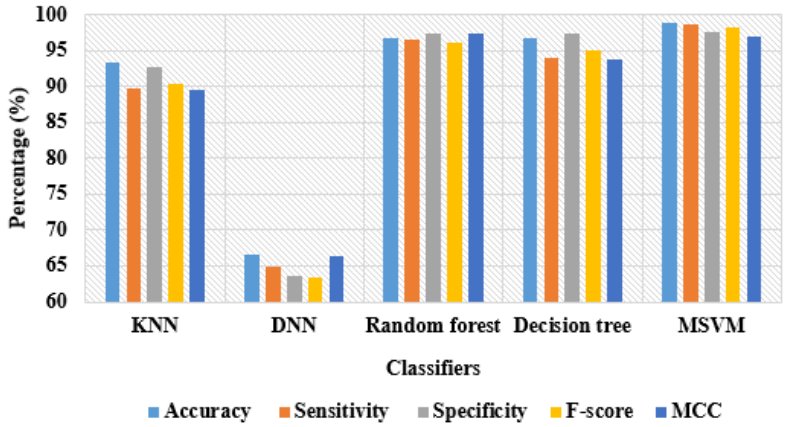

Figure. 4 The comparison result of different classifiers with MPSO algorithm

Where, FP, FN, TP and TN indicate false positive, false negative, true positive, and true negative.

4.1 Quantitative evaluation

In this scenario, the MPSO-MSVM model's effectiveness is validated on the T1-CE MRI image dataset [28], which consists of 3064 medical images in that 80:20% images are used model training and testing. In addition to this, the five-fold cross-validation is applied for more accurate estimation of the MPSO-MSVM model. In Table 1, the experimental result of different classifiers without using feature optimization is examined. By viewing

Table 3. Experimental result of different optimizers with MSVM classifier

MSVM classifier					
Optimizers	**Accuracy (%)**	**Sensitivity (%)**	**Specificity (%)**	**F-score (%)**	**MCC (%)**
GWO	93.33	93.04	93.3	93.13	92.42
BPSO	96.14	96.35	96.27	98.18	95.29
Genetic algorithm	95.07	94.78	95.53	94.78	93.81
MPSO	98.89	98.65	97.54	98.32	97.02

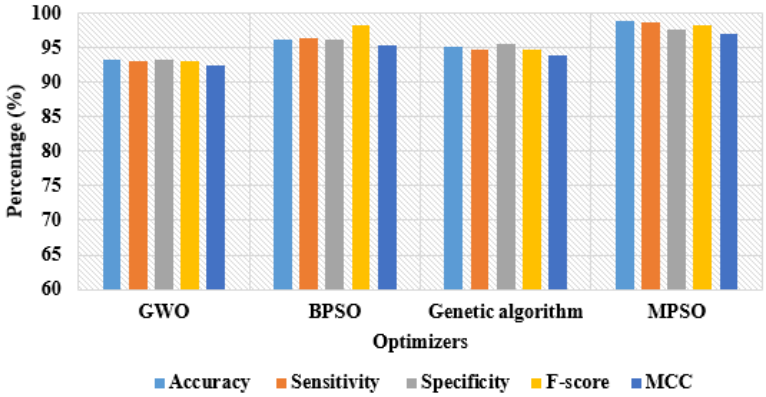

Figure. 6 Comparison result of different optimizers with MSVM classifier

Table 1, the MSVM attained maximum classification accuracy of 96.57%, specificity of 97.21%, f-score of 95.37%, sensitivity of 95.92%, and MCC of 94.48% in the brain tumor detection, which are superior compared to the existing classifiers such as KNN, deep neural network (DNN), random forest, and decision tree. The comparison result of different classifiers without using feature optimization is stated in Fig. 4.

The experimental result of different classifiers with the MPSO algorithm is examined in Table 2 in terms of MCC, specificity, sensitivity, f-score, and accuracy on the T1-CE MRI image dataset. When compared to without using the feature optimization algorithm, the classifiers with the MPSO algorithm achieved significant performance in brain tumor detection. As similar to Table 1, the MSVM classifier with MPSO algorithm obtained superior performance in MRI tumor detection compared to other classifiers such as KNN, DNN, random forest and decision tree. The MPSO-MSVM model attained maximum sensitivity of 98.65%, a classification accuracy of 98.89%, specificity of 97.54%, f-score of 98.32, and MCC of 97.02%, which are higher compared to other combinations. Hence, the comparison result of different classifiers with MPSO algorithm is stated in Fig. 5. When compared to the existing classifiers, the MSVM classifier significantly reduces resulting dual issue by creating a relaxed classification error-bound. In addition, the MSVM classifier quickly speed up the training mechanism by maintaining a competitive accuracy.

The experimental result of different optimizers with MSVM classifier is depicted in Table 3. As denoted in Table 3, the MPSO algorithm attained higher performance in MRI brain tumor detection compared to the existing optimization algorithms: grey wolf optimizer (GWO), binary particle swarm optimizer (BPSO), and genetic algorithm in light of MCC, specificity, sensitivity, f-score, and accuracy on the T1-CE MRI image dataset. The comparison result of different optimizers with MSVM classifier is denoted in Fig. 6. The inclusion of MPSO includes two key benefits such reducing training time and improving classification accuracy by eliminating the misleading features or by selecting the active features.

4.2 Comparative evaluation

The comparative investigations between the MPSO-MSVM model and the comparative models are indicated in Table 4. Swati [16] implemented the VGG-19 model for effective brain tumor detection. The VGG-19 model's effectiveness was tested on the T1-CE MRI image dataset, and the presented VGG-19 model achieved 94.82% of accuracy, 94.69% of specificity and 94.25% of sensitivity in the brain tumor detection. Díaz-Pernas [17] developed a new automated model: multiscale CNN for brain tumor segmentation and classification. The developed multiscale CNN model achieved 97.30% of accuracy and 94% of sensitivity on the T1-CE MRI image dataset. Hashemzehi [19] combined both NADE and CNN for automated brain tumor detection. The presented model achieved 95% of accuracy, 97.42%

Table 4. Comparative study between the MPSO-MSVM model and the existing models

Models	Accuracy (%)	Specificity (%)	Sensitivity (%)
VGG 19 [16]	94.82	94.69	94.25
Multiscale CNN [17]	97.30	-	94
NADE-CNN [19]	95	97.42	94.64
MPSO-MSVM	98.89	97.54	98.65

of specificity, and 94.64% of sensitivity on the T1-CE MRI image dataset. By viewing Table 4, the proposed MPSO-MSVM model obtained superior performance on T1-CE MRI image dataset in light of sensitivity, specificity and accuracy.

In the proposed model, the inclusion of the MPSO algorithm selects the discriminative feature vectors that significantly decrease the computational complexity and running time of the classifier, which are the major concerns stated in the literature section. The computational complexity of the MPSO-MSVM model is linear and the running time is 56.23 seconds, which is superior compared to other machine learning techniques.

5. Conclusion

In the computer-aided health monitoring system, brain tumor detection is a challenging task. In this manuscript, the abnormal tumors are detected by utilizing MRI, which is clear and provides precise information about the soft tissue and organ. In this manuscript, an MPSO-MSVM model is introduced for effective brain tumor detection. The MPSO-MSVM model consists of four major phases: tumor segmentation, feature extraction, optimization and tumor classification. Initially, the tumor regions are segmented using AKFCM with Otsu thresholding technique from the enhanced MRI brain images, and then the deep and texture feature vectors are extracted by employing LTP, GLCM features and LeNet-5. Next, the multidimensional extracted feature vectors are optimized by proposing an MPSO algorithm that improves the system complexity and running time. Lastly, the optimized feature values are fed to the MSVM to classify glioma, meningioma and pituitary tumor. In the resulting phase, the MPSO-MSVM model achieved classification accuracy of 98.89% on the T1-CE MRI image dataset, which is better related to the traditional classifiers and optimizers. As a future extension, a hyper-parameter optimization based deep learning model can be developed to further enhance brain tumor detection.

Conflicts of interest

The authors declare no conflict of interest.

Author contributions

The paper conceptualization, methodology, software, validation, formal analysis, investigation, resources, data curation, writing—original draft preparation, writing—review and editing, visualization, have been done by 1st author. The supervision and project administration, have been done by 2nd author.

References

[1] V. V. Kumar, K. S. Krishna, and S. Kusumavathi, "Genetic algorithm based feature selection brain tumour segmentation and classification", *International Journal of Intelligent Engineering and Systems*, Vol. 12, No. 5, pp. 214-223, 2019, doi: 10.22266/ijies2019.1031.21.

[2] S. K. Rao and B. Lingappa, "Image analysis for MRI based brain tumour detection using hybrid segmentation and deep learning classification technique", *International Journal of Intelligent Engineering and Systems*, Vol. 1, No. 2, pp. 53-62, 2019, doi: 10.22266/ijies2019.1031.06.

[3] S. T. Kebir, S. Mekaoui, and M. Bouhedda, "A fully automatic methodology for MRI brain tumour detection and segmentation", *The Imaging Science Journal*, Vol. 67, No. 1, pp. 42-62, 2019.

[4] M. Soltaninejad, G. Yang, T. Lambrou, N. Allinson, T. L. Jones, T. R. Barrick, F. A. Howe, and X. Ye, "Supervised learning based multimodal MRI brain tumour segmentation using texture features from supervoxels", *Computer methods and Programs in Biomedicine*, Vol. 157, pp. 69-84, 2018.

[5] R. B. Vallabhaneni and V. Rajesh, "Brain tumour detection using mean shift clustering and GLCM features with edge adaptive total variation denoising technique", *Alexandria Engineering Journal*, Vol. 57, No. 4, pp. 2387-2392, 2018.

[6] S. Maharjan, A. Alsadoon, P. W. C. Prasad, T. A. Dalain, and O. H. Alsadoon, "A novel enhanced softmax loss function for brain tumour detection using deep learning", *Journal of Neuroscience Methods*, Vol. 330, p. 108520, 2020.

[7] N. Arunkumar, M. A. Mohammed, S. A. Mostafa, D. A. Ibrahim, J. J. Rodrigues, and V. H. C. D. Albuquerque, "Fully automatic model-based segmentation and classification approach for MRI brain tumor using artificial neural networks", *Concurrency and Computation:*

Practice and Experience, Vol. 32, No. 1, p. e4962, 2020.

[8] A. Pinto, S. Pereira, D. Rasteiro, and C.A. Silva, "Hierarchical brain tumour segmentation using extremely randomized trees", *Pattern Recognition*, Vol. 82, pp. 105-117, 2018.

[9] Z. U. Rehman, S. S. Naqvi, T. M. Khan, M. A. Khan, and T. Bashir, "Fully automated multi-parametric brain tumour segmentation using superpixel based classification", *Expert Systems with Applications*, Vol.118, pp. 598-613, 2019.

[10] G. S. Tandel, A. Balestrieri, T. Jujaray, N. N. Khanna, L. Saba, and J. S. Suri, "Multiclass magnetic resonance imaging brain tumor classification using artificial intelligence paradigm", *Computers in Biology and Medicine*, Vol. 122, p. 103804, 2020.

[11] O. N. Belaid, and M. Loudini, "Classification of Brain Tumor by Combination of Pre-Trained VGG16 CNN", *Journal of Information Technology Management*, Vol. 12, No. 2, pp. 13-25, 2020.

[12] S. Deepak, and P. M. Ameer, "Brain tumor classification using deep CNN features via transfer learning", *Computers in Biology and Medicine*, Vol. 111, p. 103345, 2019.

[13] S. Anjum, L. Hussain, M. Ali, M. H. Alkinani, W. Aziz, S. Gheller, A. A. Abbasi, A. R. Marchal, H. Suresh, and T. Q. Duong, "Detecting brain tumors using deep learning convolutional neural network with transfer learning approach", *International Journal of Imaging Systems and Technology*, Vol. 32, No. 1, pp. 307-23, 2021.

[14] G. Li, J. Sun, Y. Song, J. Qu, Z. Zhu, and M. R. Khosravi, "Real-time classification of brain tumors in MRI images with a convolutional operator-based hidden Markov model", *Journal of Real-Time Image Processing*, Vol. 18, pp. 1207–1219, 2021.

[15] S. Tripathi, A. Verma, and N. Sharma, "Automatic segmentation of brain tumour in MR images using an enhanced deep learning approach", *Computer Methods in Biomechanics and Biomedical Engineering: Imaging & Visualization*, Vol. 9, No. 2, pp. 121-130, 2021.

[16] Z. N. K. Swati, Q. Zhao, M. Kabir, F. Ali, Z. Ali, S. Ahmed, and J. Lu, "Brain tumor classification for MR images using transfer learning and fine-tuning", *Computerized Medical Imaging and Graphics*, Vol. 75, pp. 34-46, 2019.

[17] F. J. D. Pernas, M. M. Zarzuela, M. A. Rodríguez, and D. G. Ortega, "A deep learning approach for brain tumor classification and segmentation using a multiscale convolutional neural network", *In Healthcare, Multidisciplinary Digital Publishing Institute*, Vol. 9, No. 2, p. 153, 2021.

[18] H. H. Sultan, N. M. Salem, and W. A. Atabany, "Multi-Classification of Brain Tumor Images Using Deep Neural Network", *IEEE Access*, Vol. 7, pp. 69215-69225, 2019.

[19] R. Hashemzehi, S. J. S. Mahdavi, M. Kheirabadi, and S. R. Kamel, "Detection of brain tumors from MRI images base on deep learning using hybrid model CNN and NADE", *Biocybernetics and Biomedical Engineering*, Vol. 40, No. 3, pp. 1225-1232, 2020.

[20] K. Kaplan, Y. Kaya, M. Kuncan, and H. M. Ertunç, "Brain tumor classification using modified local binary patterns (LBP) feature extraction methods", *Medical Hypotheses*, Vol. 139, p. 109696, 2020.

[21] S. A. A. Ismael, A. Mohammed, and H. Hefny, "An enhanced deep learning approach for brain cancer MRI images classification using residual networks", *Artificial Intelligence in Medicine*, Vol. 102, p. 101779, 2020.

[22] D. Rammurthy and P. K. Mahesh, "Whale Harris Hawks optimization based deep learning classifier for brain tumor detection using MRI images", *Journal of King Saud University-Computer and Information Sciences*, In Press, 2020.

[23] B. Srikanth and S. V. Suryanarayana, "Multi-Class classification of brain tumor images using data augmentation with deep neural network", *Materials Today: Proceedings*, In Press, 2021.

[24] P. A. T. Hapsari, J. R. Dewinda, V. A. Cucun, Z. F. Nurul, S. Joan, D. S. Anggraini, M. A. Peter, E. P. I. Ketut, and H. P. Mauridhi, "Brain Tumor Classification in MRI Images Using En-CNN", *International Journal of Intelligent Engineering and Systems*, Vol. 14, No. 4, pp. 437-451, 2021, doi: 10.22266/ijies2021.0831.38.

[25] O. A. M. F. Alnaggar, B. N. Jagadale, and S. H. Narayan, "MRI Brain Tumor Detection Using Boosted Crossbred Random Forests and Chimp Optimization Algorithm Based Convolutional Neural Networks", *International Journal of Intelligent Engineering and Systems*, Vol. 15, No. 2, pp. 36-46, 2022, doi: 10.22266/ijies2022.0430.04.

[26] N. Ghassemi, A. Shoeibi, and M. Rouhani, "Deep neural network with generative adversarial networks pre-training for brain tumor classification based on MR images", *Biomedical Signal Processing and Control*, Vol. 57, p. 101678, 2020.

[27] G. Hu, and Z. Du, "Adaptive kernel-based fuzzy c-means clustering with spatial constraints for image segmentation", *International Journal of Pattern Recognition and Artificial Intelligence*, Vol. 33, No. 1, pp. 1954003, 2019.
[28] T1-CE MRI dataset: https://figshare.com/articles/dataset/brain_tumor_dataset/1512427